

# An Experimental and CFD Analysis on Heat Transfer and Fluid Flow Characteristics of a Tube Equipped with X-Shaped Tape Insert in a U-Shaped Heat Exchanger



Sagar Paneliya, Sakshum Khanna, Jeet Mehta, Vishal Kathiriya, Umang Patel, Parth Prajapati, and Indrajit Mukhopdhyay

## 1 Introduction

Heat exchanger is simply one of the most important and widely used process equipments found in industrial sites [1]. It opens up the possibilities for application in industries like refrigeration, air-conditioning [2], production of electricity at nuclear and thermal power plants, automotives and many more. Hence, finding ways and means to improve thermal performance are of great importance. High-performance heat transfer system (HTS) holds an important role in the majority of industrial applications. Heat transfer can be carried out by either active HTS or passive HTS. Active HTS methods use external means to promote heat transfer such as electromagnetic fields, surface vibration and spray atomizer. Active HTS requires external power source depending on end applications, and hence, power cost should be taken into consideration during selection of active HTS [3].

To overcome the challenges of active HTS, passive techniques are introduced, which provide heat transfer enhancement at low cost without the use of external power source. One of the widely accepted techniques is to use insert tapes of different configurations. Several experimental investigations has been performed to enhance heat transfer using various types of insert such as mesh, strip, wire, coil, twisted tapes and helical insert. There have been several experimental investigations of the

---

S. Paneliya · S. Khanna · J. Mehta · V. Kathiriya · I. Mukhopdhyay (✉)  
Department of Solar Energy, Pandit Deendayal Petroleum University, Raysan, Gandhinagar,  
Gujarat 382007, India  
e-mail: [Indrajit.m@sse.pdpu.ac.in](mailto:Indrajit.m@sse.pdpu.ac.in)

U. Patel  
Department of Mechanical Engineering, SVBIT, Vasan, Gujarat, India

P. Prajapati  
Department of Mechanical Engineering, Pandit Deendayal Petroleum University, Raysan,  
Gandhinagar, Gujarat 382007, India

heat exchanger tube with insert that showed higher heat transfer rate, friction factor and effectiveness than the plain tube. Halit Bas et al. [4], in 2012, experimentally investigated heat transfer enhancement in a tube fitted with twisted tape insert. They concluded that the twist ratio ( $Y/D$ ) plays a significant role as compared to clearance ratio ( $C/D$ ) for heat transfer enhancement. For the same clearance ratio of 0.0178 and varying twist ratio of 2, 2.5, 3, 3.5 and 4, heat transfer enhancement of 1.75, 1.70, 1.64, 1.60 and 1.58, respectively, was achieved. Hence, increase in Reynolds number due to increase in twist ratio leads to decrease in heat transfer enhancement. Heat transfer enhancement was found to be higher for  $C/D = 0.0178$  than  $C/D = 0.0357$  for all twist ratios. A similar study on the thermal performance of a heat exchanger was carried out by Eiamsa-ard et al. [5] with regularly spaced twisted tape inserts. These inserts were used to generate swirl in the heat exchanger tube. They found out that full length twisted tape insert ( $s = 0$ ) provided higher heat transfer rate, friction factor and thermal performance than regularly spaced twisted tape insert ( $s = 1.0, 2.0, 3.0$ ). For the same twist ratio, the twisted tape insert with different space ratio,  $s = 0, 1.0, 2.0$  and  $3.0$ , gave enhancement of heat transfer of 56.8%, 46.2%, 30.5% and 22.6% and friction factor of 4.22, 3.78, 3.17 and 2.63 times, respectively, when compared with plain tube. Hence, increase in space ratio decreases the augmented heat transfer, friction factor and thermal performance. They also concluded that increase in twist ratio decreases the augmented heat transfer and friction factor.

Objective of this chapter is to determine the heat transfer and pressure drop characteristics of turbulent flow in the pipes fitted with X-shaped tape insert for a U-shaped tube heat exchanger. The operational performance of the tube incorporated with X-shaped tape insert was compared theoretically through CFD modelling for variable mass flow rates of cold and hot water. In this chapter, Sect. 2 illustrates and explains the experimental set-up and the thermal model of the heat exchanger. Section 3 compares the results obtained for the heat exchanger with and without X-shaped insert experimentally, and the results are then verified with CFD values. Finally, Sect. 4 concludes the experiment and major findings.

## 2 Experimental Section

In this section, test setup of the U-shaped heat exchanger established to conduct the experiments is discussed and reported. Figure 1 depicts the experimental setup of the test section along with sensors and controller mounted on the system. The cold water was supplied from an overhead tank to the inner annulus of the U-shaped tube, and the water was drained out into the underground tank. Constant flow rate of water was maintained by the overhead tank. The hot water was supplied in the counter-flow direction within the outer annulus of the U-shaped tube by a centrifugal pump. Wooden flanges served as the support structure for the tube. The test section was fitted with X-shaped tape insert during the experiment to observe the heat transfer enhancement. Individual section plates of dimension 1000 mm  $\times$  8 mm  $\times$  3 mm

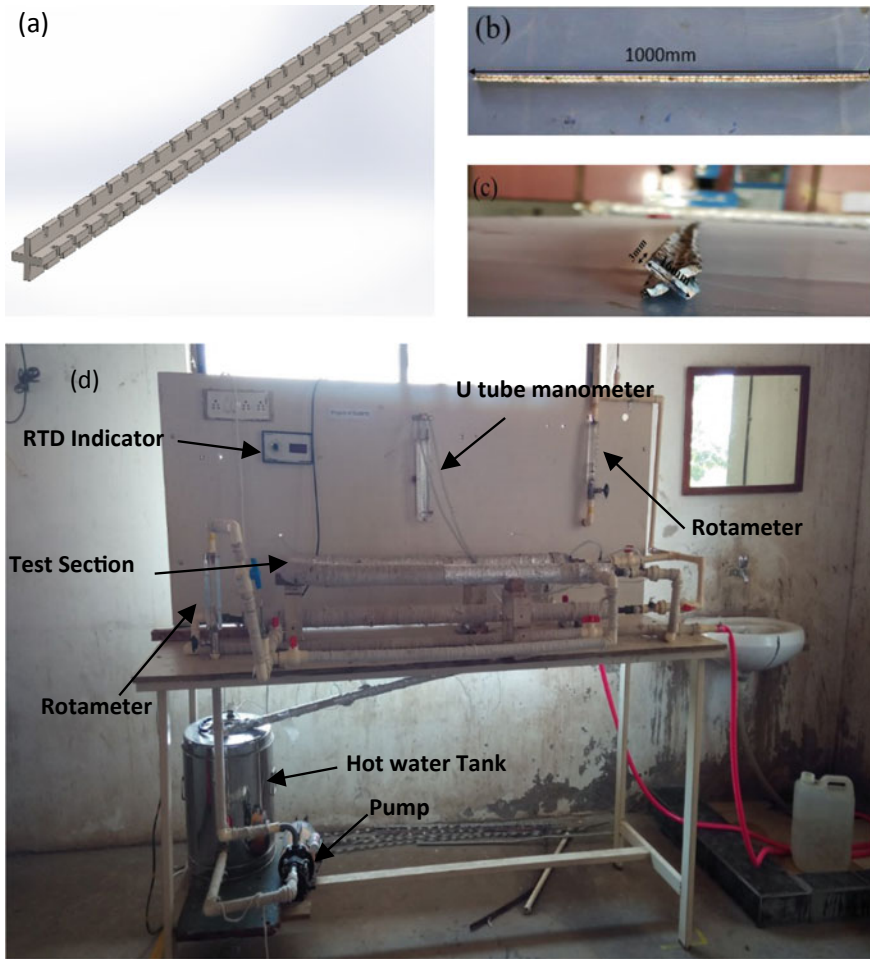


**Fig. 1** a Detail view of X tape. b X-shaped tape insert employed in the tube top view. c X-shaped tape insert employed in the tube front view. d The experimental setup

were joined together at 90° using spot welding, thus forming an X-shaped tape insert as shown in Fig. 1b. Longitudinal slots along the length of the insert were created to incorporate turbulence to the flow and increase the surface area. Furthermore, the edges of the slots were filed for a proper surface roughness. Material used for the fabrication of the insert was mild steel. Temperatures at various intermittent sections of the U-shaped tube were measured by resistant temperature detectors (RTD).

Pressure drop of water across the tube was measured by U-tube manometer. Rotameter was used to measure and regulate mass flow rate of water. Heat transfer loss to the surroundings was minimized by a layer of asbestos thread and aluminium foil wrapped around the U-shaped tube. The heat transfer characteristics of water

flowing through concentric tube of U-shaped tube heat exchanger fitted with and without the X-shaped insert has been investigated. Counter-flow configuration for the heat exchanger was used in the test section for the working fluid. The hot water was supplied at 70 °C at constant mass flow rate of 40, 50 and 60 LPH for different experiments. While cold water was supplied at 38 °C, its mass flow rate was varied from 40 to 140 LPH in the regular interval of 20 LPH.

## 2.1 Thermal Model

Well-developed heat transfer correlations were used to determine the heat transfer rate in the heat exchanger.

$$Q = mC_p(T_{co} - T_{ci}) \quad (1)$$

Logarithmic mean temperature difference (LMTD) of water at inlet and outlet was calculated by using Eq. 2.

$$\text{LMTD} = \frac{(T_{ho} - T_{ci}) - (T_{hi} - T_{co})}{\ln \frac{T_{ho} - T_{ci}}{T_{hi} - T_{co}}} \quad (2)$$

where  $T_{ho}$ ,  $T_{hi}$ ,  $T_{co}$ ,  $T_{ci}$  are the temperatures of hot and cold water at outlet and inlet of the U-shaped tube, respectively. Overall heat transfer coefficient, Nusselt number, effectiveness and friction factor was calculated by using Eq. (3)–(11).

$$U = \frac{Q}{A \times \text{LMTD}} \quad (3)$$

$$\mu = \left(3 \times 10^{-8} \times T_{\text{avg}}^4\right) - \left(9 \times 10^{(-6)} \times T_{\text{avg}}^3\right) + \left(0.001 \times T_{\text{avg}}^2\right) - \left(0.058 \times T_{\text{avg}}\right) + 1.778 \quad (4)$$

$$v = \frac{4m_{co}}{\pi \times d_i^2} \quad (5)$$

$$\text{Pr} = \frac{\mu \times Cp}{K} \quad (6)$$

$$\text{Re} = \frac{1000 \times V \times d_i}{\mu} \quad (7)$$

$$\text{Nu} = 0.023 * (\text{Re}^{0.8}) * (\text{Pr}^{0.4}) \quad \text{for Re} < 4000 \quad (8)$$

$$\text{Nu} = 0.023 * (\text{Re}^{0.8}) * (\text{Pr}^{0.33}) \quad \text{for Re} > 4000 \quad (9)$$

$$\varepsilon = \frac{Q}{C_{\min}(T_{hi} - T_{co})} \tag{10}$$

$$f = \frac{\Delta P}{\left(\frac{L}{D}\right)\left(\frac{\rho U^2}{2}\right)} \tag{11}$$

### 3 Results and Discussion

#### 3.1 Experimental Results

The experimental investigation was undertaken to study the heat transfer characteristics of U-shaped tube fitted with and without X-shaped tape insert. The experiments were performed with variable mass flow rates of cold water for a constant mass flow rate of hot water within the tube. The augmented heat transfer rate and overall heat transfer coefficient for variable mass flow rate of cold water is shown in Figs. 2 and 3, respectively. Similarly, results are recorded for three different flow rates (40, 50, 60 LPH) of hot water. As heat transfer rate is mainly dependent on specific heat capacity and mass flow rate of water, it was evident that the heat transfer rate was found to be considerably high for tube fitted with X-shaped insert as compared to tube without the insert. Results showed that maximum heat transfer rate and overall heat transfer coefficient of 1463 W and 639.58 W/m<sup>2</sup>K, respectively, was achieved at flow rate of 140 LPH of cold water and 40 LPH of hot water. Compared to tube without insert, maximum increase in heat transfer rate and overall heat transfer coefficient of 2.5 times and 3.15 times, respectively.

**Fig. 2** Plotted graph between heat transfer rate ( $Q$ ) and variable mass flow rate (LPH) of cold water for different mass flow rates of hot water for X-shaped tape insert

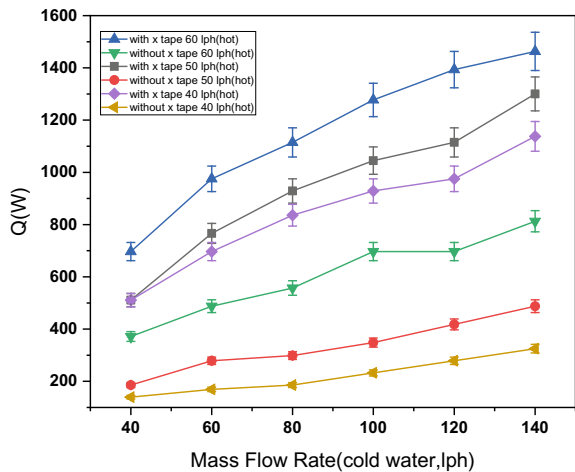
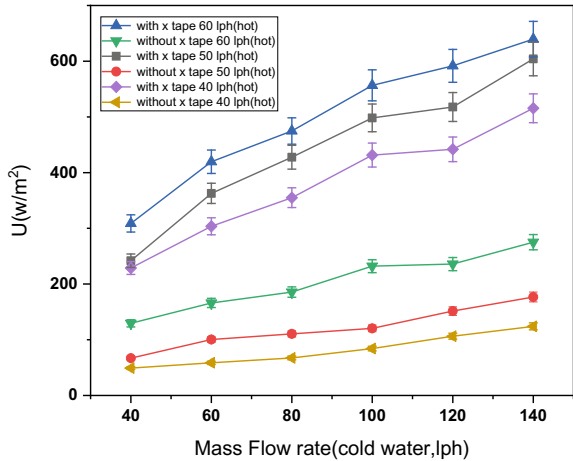


**Fig. 3** Plotted graph between overall heat transfer coefficient ( $U$ ) and variable mass flow rate (LPH) of cold water for different mass flow rates of hot water for X-shaped tape insert



The augmentation of heat transfer rate and overall heat transfer coefficient due to the incorporation of X-shaped insert in the U-shaped tube is discernible due to the turbulence created by insert which again increases with increase in mass flow rate.

Performance of heat transfer system was characterized by its effectiveness of heat transfer. The effectiveness ( $\epsilon$ ) is defined as the ratio of actual heat transfer rate to maximum heat transfer rate. The variation of effectiveness ( $\epsilon$ ) with mass flow rate of cold water is shown in Fig. 4. Effectiveness was measured for three different flow rates of hot water. As evident from the graph, the  $\epsilon$  is larger in a U-shaped tube with X-shaped insert as compared to the plain U-shaped tube. Results showed that maximum effectiveness of 0.83 was achieved for tube fitted with X-shaped tape insert at flow rate of 40 LPH of cold water and 60 LPH of hot water.

**Fig. 4** Plotted graph between effectiveness ( $\epsilon$ ) and variable mass flow rate (LPH) of cold water for different mass flow rates of hot water

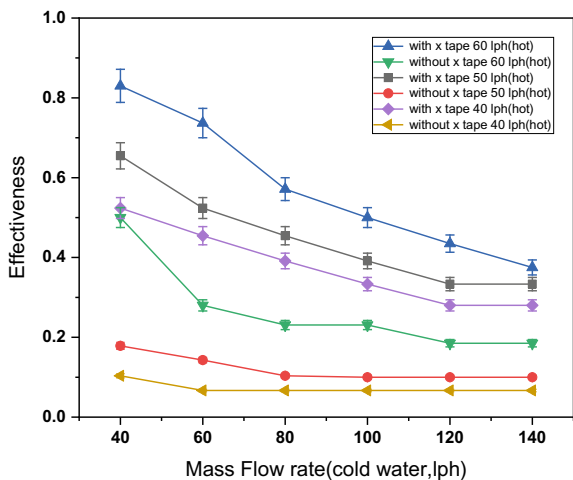
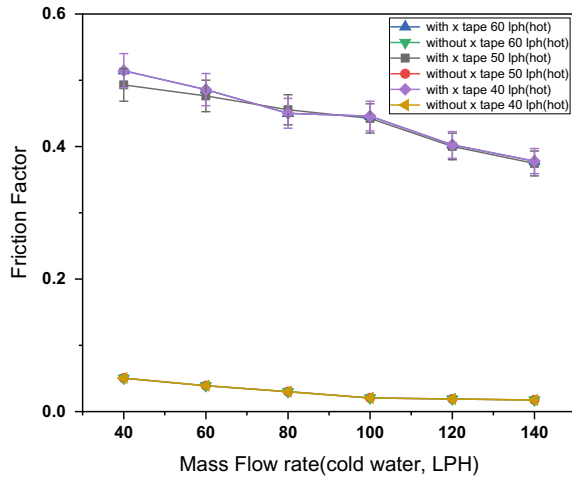


**Fig. 5** Plotted graph friction factor ( $f$ ) between and variable mass flow rate (LPH) of cold water for different mass flow rates of hot water for X-shaped tape insert



Moreover, it can be observed that the effectiveness decreases with the increase in mass flow rate of cold water at a given mass flow rate of hot water. The variation of friction factor with mass flow rate of cold water is shown in Fig. 5. As expected, significantly higher values of friction factor were observed for a tube fitted with X-shaped tape insert as compared to the plain tube. It was also observed that the friction factor decreased with increase in mass flow rate of cold water. Minimum friction factor of 0.386 was observed for the tube fitted with X-shaped tape insert at flow rate of 140 LPH of cold water. Increase in the turbulence and blocking effect due to X-shaped tape at the insert wall account for such observations.

### 3.2 Modelling Results

Present-day fluid mechanical complications cannot be solved without the use of computational fluid dynamics (CFD). CFD software gives the authority to simulate flows of gases and liquids, heat and mass transfer, etc. The software can also help to build a virtual prototype before it can be applied in the real world. The images and data obtained can predict the performance of the system. Computer software can help in simulating the interaction of fluids with the complex surfaces used in engineering applications. CFD simulation was carried out for the U-shaped tube with and without the insert. The temperature and pressure difference across the tube were measured at various mass flow rates of cold water which were then verified with data obtained from numerical modelling as shown in Tables 1, 2, 3 and 4. The measured and the computational results were found to be in reasonable agreement to each other. From Tables 1 and 2, it can be inferred that the average temperature of cold water was higher when the plain U-shaped pipe is fitted with X-shaped tape insert. Similarly, it can be inferred from Table 3 and 4, that the pressure drop is more when X-shaped

**Table 1** Predicted and measured average temperature of cold water without insert

MFR (LPH) cold water	40 LPH (hot water)			50 LPH (hot water)			60 LPH (hot water)		
	$T_{avg}$ (CFD), °C	$T_{avg}$ (Exp), °C	Error (%)	$T_{avg}$ (CFD), °C	$T_{avg}$ (Exp), °C	Error (%)	$T_{avg}$ (CFD), °C	$T_{avg}$ (Exp), °C	Error (%)
40	40.795	39.5	3.28	41.41	40	3.53	42.985	42	2.35
60	40.4	39	3.59	40.99	40	2.48	42.545	41.5	2.52
80	39.795	39	2.04	40.56	39.5	2.68	42.12	41	2.73
100	39.97	39	2.49	39.545	38.5	2.71	41.845	41	2.06
120	39.96	39	2.46	39.485	38.5	2.56	41.32	40.5	2.02
140	39.74	39	1.9	39.385	38.5	2.3	41.355	40.5	2.11

Without X-shaped



**Table 2** Predicted and measured average temperature of cold water with insert

MFR (LPH) cold water	40 LPH (hot water)			50 LPH (hot water)			60 LPH (hot water)		
	$T_{avg}$ (CFD), °C	$T_{avg}$ (Exp), °C	Error (%)	$T_{avg}$ (CFD), °C	$T_{avg}$ (Exp), °C	Error (%)	$T_{avg}$ (CFD), °C	$T_{avg}$ (Exp), °C	Error (%)
40	44.485	43.5	2.26	44.76	43.5	2.9	46.03	44.5	3.44
60	44.885	43	4.38	44.43	43.5	2.14	45.075	44	2.44
80	43.425	42.5	2.18	43.935	43	2.17	44.195	43	2.78
100	42.93	42	2.21	43.44	42.5	2.21	43.58	42.5	2.54
120	42.56	41.5	2.55	42.995	42	2.37	42.97	42	2.31
140	42.61	41.5	2.67	42.925	42	2.20	42.69	41.5	2.87

With X-shaped

**Table 3** Predicted and measured pressure drop across the test section without insert

MFR (LPH) cold water	40 LPH (hot water)			50 LPH (hot water)			60 LPH (hot water)		
	$\Delta P$ (CFD), N/m <sup>2</sup>	$\Delta P$ (Exp), N/m <sup>2</sup>	Error (%)	$\Delta P$ (CFD), N/m <sup>2</sup>	$\Delta P$ (Exp), N/m <sup>2</sup>	Error (%)	$\Delta P$ (CFD), N/m <sup>2</sup>	$\Delta P$ (CFD), N/m <sup>2</sup>	Error (%)
40	2.279	2.401	5.043	2.279	2.465	7.512	2.279	2.404	5.181
60	4.029	4.250	5.212	4.029	4.323	6.811	4.029	4.323	6.811
80	5.677	5.959	4.725	5.677	6.051	6.172	5.677	6.061	6.329
100	6.185	6.479	4.545	6.185	6.479	4.545	6.185	6.479	4.545
120	8.270	8.906	7.143	8.270	8.889	6.967	8.270	9.091	9.034
140	10.275	10.568	2.773	10.275	11.111	7.529	10.275	11.111	7.529

Without X-shaped

**Table 4** Predicted and measured pressure drop across the test section with insert

MFR (LPH) cold water	40 LPH (hot water)			50 LPH (hot water)			60 LPH (hot water)		
	$\Delta P$ (CFD), N/m <sup>2</sup>	$\Delta P$ (Exp), N/m <sup>2</sup>	Error (%)	$\Delta P$ (CFD), N/m <sup>2</sup>	$\Delta P$ (Exp), N/m <sup>2</sup>	Error (%)	$\Delta P$ (CFD), N/m <sup>2</sup>	$\Delta P$ (CFD), N/m <sup>2</sup>	Error (%)
40	22.847	23.129	1.217	22.847	23.264	1.794	22.847	23.264	1.794
60	48.969	51.165	4.292	48.969	52.345	6.449	48.969	50.242	2.534
80	81.806	87.110	6.089	81.806	86.040	4.922	81.806	86.476	5.401
100	124.689	127.787	2.424	124.689	129.404	3.643	124.689	129.356	3.608
120	160.398	170.798	6.089	160.398	166.170	3.474	160.398	173.442	7.521
140	209.642	221.139	5.199	209.642	223.204	6.076	209.642	222.768	5.892

With X-shaped

insert is used. These results show the augmentation of heat transfer rate and overall heat transfer coefficient when the X-shaped tape insert is incorporated in the heat exchanger.

Tables 5 and 6 show the results and percentage error of the values of Nusselt number obtained for various mass flow rates of cold water. The results obtained for different mass flow rates of cold water shows increase in Nusselt number with increase in mass flow rate. Also, with the incorporation of X-shaped tape insert the further increase in Nusselt number is observed. This eventually leads to the increase in heat transfer rate and overall heat transfer coefficient of the system. In addition, from Tables 7 and 8 it is evident that the friction factor increases considerably by the addition of X-shaped insert in the U-shaped tube. Figure 6 shows CFD simulation of the pressure and temperature distribution profile of the heat exchanger, respectively.

## 4 Conclusion

In conclusion, the heat transfer characteristics of a heat exchanger were studied for the U-shaped tube fitted with an X-shaped tape insert. Experiments were performed for different flow rates of hot and cold water passing through the heat exchanger. The results obtained from the experiment were substantiated with results of the computational fluid dynamics simulation. Experimental results obtained showed the conclusive proof of augmentation of heat transfer rate and overall heat transfer coefficient. The incorporation of X-shaped tape showed maximum enhancement of heat transfer rate and overall heat transfer coefficient of 2.5 and 3.15 times, respectively, as compared to the U-shaped tube at 40 LPH of hot water and 140 LPH of cold water. It was observed that with increase in flow rate of cold water (inside the tube), increases the turbulence due to the X-shaped tape insert. Hence, the turbulence created by the presence of X-shaped insert has to be one of the main reasons for enhancement of heat transfer rate. The simulated results were found in proper agreement with the experimental results having an error in the range from 2 to 5%.

## 5 Authors Information

The manuscript was written through contributions of all authors. All authors have given approval to the final version of the manuscript.

**Table 5** Predicted and calculated Nusselt number of the cold water without insert

MFR (LPH) cold water	40 LPH (hot water)			50 LPH (hot water)			60 LPH (hot water)		
	Nu (CFD)	Nu (Exp)	Error (%)	Nu (CFD)	Nu (Exp)	Error (%)	Nu (CFD)	Nu (Exp)	Error (%)
	40	10.540	10.730	1.773	10.579	10.782	1.882	10.830	10.991
60	14.492	14.769	1.878	14.693	14.913	1.475	14.900	15.130	1.523
80	18.166	18.591	2.288	18.207	18.682	2.544	18.519	18.955	2.298
100	21.901	22.225	1.458	21.777	22.116	1.533	22.379	22.659	1.236
120	22.905	23.447	2.309	22.716	23.313	2.558	23.287	23.851	2.363
140	26.186	26.524	1.275	25.989	26.372	1.454	26.577	26.981	1.500

Without X-shaped

**Table 6** Predicted and measured Nusselt number of the cold water with insert

MFR (LPH) cold water	40 LPH (hot water)			50 LPH (hot water)			60 LPH (hot water)		
	Nu (CFD)	Nu (Exp)	Error (%)	Nu (CFD)	Nu (Exp)	Error (%)	Nu (CFD)	Nu (Exp)	Error (%)
40	10.997	11.150	1.366	10.958	11.150	1.724	11.033	11.256	1.980
60	15.152	15.349	1.281	15.249	15.422	1.124	15.285	15.495	1.356
80	18.818	19.229	2.138	18.854	19.321	2.415	18.862	19.321	2.377
100	22.554	22.877	1.412	22.661	22.987	1.420	22.674	22.987	1.363
120	23.514	24.122	2.519	23.720	24.258	2.219	23.672	24.258	2.416
140	26.827	27.288	1.689	27.067	27.442	1.366	26.864	27.288	1.553

**Table 7** Predicted and measured friction factor of the cold water without insert

MFR (LPH) cold water	40 LPH (hot water)			50 LPH (hot water)			60 LPH (hot water)		
	$F$ (CFD)	$f$ (Exp)	Error (%)	$f$ (CFD)	$F$ (Exp)	Error (%)	$F$ (CFD)	$f$ (Exp)	Error (%)
40	0.048	0.051	5.043	0.048	0.052	7.512	0.048	0.051	5.181
60	0.038	0.040	5.212	0.038	0.041	6.811	0.038	0.041	6.811
80	0.030	0.032	4.725	0.030	0.032	6.172	0.030	0.032	6.329
100	0.021	0.022	4.545	0.021	0.022	4.545	0.021	0.022	4.545
120	0.020	0.021	7.143	0.020	0.021	6.967	0.020	0.021	9.034
140	0.018	0.018	2.773	0.018	0.019	7.529	0.018	0.019	7.529

Without X-shaped

**Table 8** Predicted and measured friction factor of the cold water with insert

MFR (LPH) cold water	40 LPH (hot water)			50 LPH (hot water)			60 LPH (hot water)		
	$f$ (CFD)	$f$ (Exp)	Error (%)	$f$ (CFD)	$f$ (Exp)	Error (%)	$F$ (CFD)	$f$ (Exp)	Error (%)
40	0.485	0.491	1.217	0.485	0.494	1.794	0.485	0.494	1.794
60	0.462	0.483	4.292	0.462	0.494	6.449	0.462	0.474	2.534
80	0.434	0.462	6.089	0.434	0.456	4.922	0.434	0.459	5.401
100	0.423	0.434	2.424	0.423	0.439	3.643	0.423	0.439	3.608
120	0.378	0.403	6.089	0.378	0.392	3.474	0.378	0.409	7.521
140	0.363	0.383	5.199	0.363	0.387	6.076	0.363	0.386	5.892

Without X-shaped



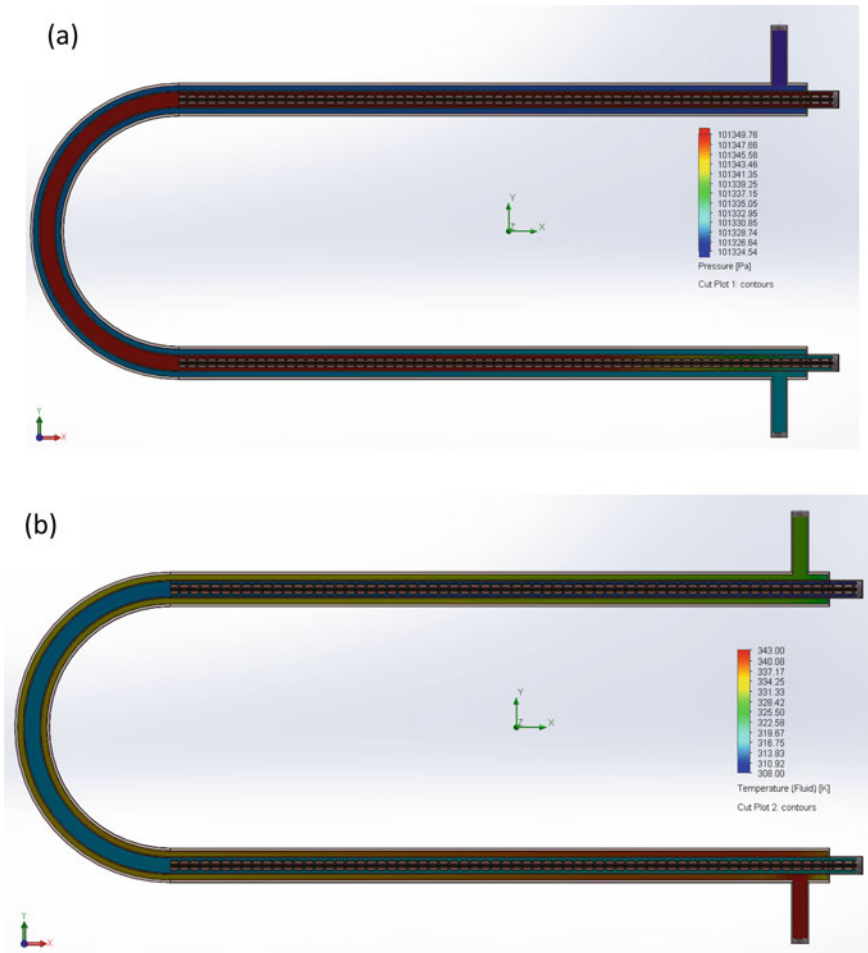


Fig. 6 a Pressure distribution and b temperature distribution of the fluid with insert

## References

1. Bergles, A.E.: ExHFT for fourth generation heat transfer technology. *Exp. Thermal Fluid Sci.* **26**, 335–344 (2002)
2. Yu, L., Liu, D.: Study of the thermal effectiveness of laminar forced convection of nanofluids for liquid cooling applications. *IEEE Trans. Compon. Packag. Manuf. Technol.* **3**, 1693–1704 (2013)
3. Gholamalizadeh, E., et al.: Study of intensification of the heat transfer in helically coiled tube heat exchangers via coiled wire insert. *Int. J. Therm. Sci.* **141**, 72–83 (2019)

4. Halit Bas, V.: Ozceyhan, Heat transfer enhancement in a tube with twisted tape insert placed separately from the tube wall. *Exp. Thermal Fluid Sci.* **41**, 51–58 (2012)
5. Eiamsa-ard, P., Piriyaungroj, N., Thianpong, C., Eiamsa-ard, S.: A case study on thermal performance assessment of a heat exchanger tube equipped with regularly-spaced twisted tapes as swirl generators. *Case Stud. Therm. Eng.* **3**, 86–102 (2014)